

# Twins in asymmetrically rolled AZ31 analyzed with a Transmission Electron Microscope Orientation mapping tool

**E F Rauch, M Forget, G Kapelski**

Science et Ingénierie des Matériaux et des Procédés, Université de Grenoble/CNRS, Grenoble INP–UJF, 38402 Saint-Martin d’Hères, France

E-mail: edgar.rauch@simap.grenoble-inp.fr

**Abstract.** An AZ31 sheet was rolled in symmetrical and asymmetrical conditions to a total reduction of 50%. Twins and double twins are the dominant structural features observed after deformation. They were analyzed systematically with the help of a dedicated TEM attachment that provides orientation maps at nanoscale. This particular characterization technic is similar to SEM-EBSD tools but far less sensitive to strains. Twinning is shown to differ substantially with the introduction of a shear component. Despite their frequency, it is argued that twins have little effect on the forming process.

**Key Words:** Asymmetrical rolling, magnesium alloys, ACOM-TEM, twinning, double twins

## 1. Introduction

Magnesium alloys are becoming major materials for the production of light structural parts. However, their use is restricted by their relatively poor ductility in cold forming. For rolled sheets, part of this limitation is due to the strong anisotropy that, in turns, is related to the intense {0002} texture. It has been reported that a final deformation step through asymmetrical rolling modifies the texture and improves the deep drawability of magnesium alloys [1]. The present project intends to analyze the structural evolution related to the shear component introduced by asymmetrical rolling on an AZ31 alloy.

The structural state of highly deformed metallic materials are hard to characterize with a transmission electron microscope (TEM). This is particularly true for severely deformed materials but even for moderate to high strains - as in rolling - TEM bright field micrographs are unable to distinguish unambiguously grain boundaries from cell boundaries. A TEM tool was developed to capture the essential characteristics of severely deformed materials [2]. The resulting attachment acquires full series of diffraction patterns and extracts both orientation and phases out of the diffracting signal. To that respect, it is similar to EBSD accessory but adapted to TEMs and provides an improved spatial resolution with respect to SEMs counterparts. The resulting so-called Automated Crystal Orientation Mapping (ACOM-TEM) technique is currently more used in the fields of nano-materials for phase recognition than for its initial purpose that was orientation mapping on deformed metallic samples. It is the objective of the present work to describe the approach and to illustrate its potentialities through the characterization of the structural state of asymmetrically rolled magnesium alloy. In particular, the twin system activities will be analyzed.

## 2. The Automated Crystal Orientation Mapping (ACOM) strategy

Electron backscatter diffraction (EBSD) attachments for scanning electron microscopes (SEM) have become essential structural characterization tools for material sciences. The technique has continuously been improved during the last decades. It nevertheless suffers from inherent limitations: in particular, the Kikuchi lines, used to extract phase or orientation information, are known to fade away if plastic deformation increases.

Similar approaches were proposed for Transmission Electron Microscopes (TEM) with the clear objective to gain in spatial resolution [3, 4]. Indeed, the latter is expected to scale with



the probe size and a FEG equipped Transmission Electron Microscopes is known to provide proper diffraction signal with a beam diameter of 1 nm or less. Most of these attempts uses Kikuchi lines as EBSD tools and, therefore, suffer the same decrease of signal with increasing strain as the SEM accessory.

The Bragg spots contained in TEM diffraction patterns also enclose phase and crystallographic orientation information and are reliable even for severely deformed materials. Orientations and phases are extracted automatically from the pattern with a dedicated approach that makes use of a template matching algorithm [5, 6]. Basically, the idea is to invert the identification problem by comparing the collected image to templates that were pre-calculated for all possible orientations of the expected phases rather than deducing ab-initio the crystallographic planes that may be related to the observed diffracting spots (Fig.1). This approach initially developed for cubic materials was extended to any kind of crystallographic structure – including hexagonal lattices - by adapting the template generation software.

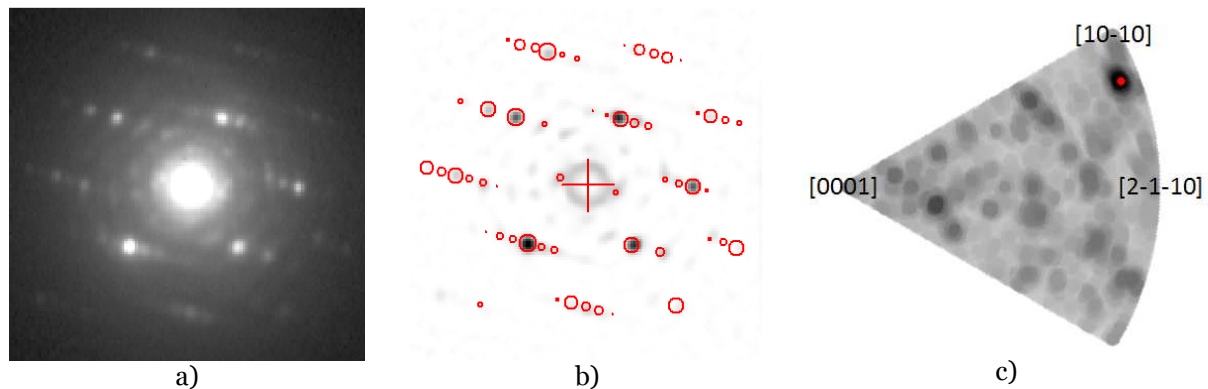


**Figure 1:** Template matching. The diffraction pattern (a) has been compared to the pre-calculated templates (red spots in b). The matching index is given for all templates in grey scale in the relevant fraction of the stereographic projection (c). The most probable solution is highlighted.

The identification algorithm uses both beam position and intensity. The strong sensitivity of the latter to so-called dynamical effects usually decreases the indexing capability of the tool. To overcome this limitation, the template matching identification approach was coupled to electron precession. The reflection intensities in diffraction patterns obtained with precession are closer to the predictions of the kinematical theory. The templates are themselves calculated without dynamical effects. This leads to a substantial increase in the image identification capability of the pattern matching software. The resulting tool turns out to be a fast and efficient crystal phase and orientation indexing attachment for TEM [2] similar and complementary to the widespread EBSD equipment for SEM.

### 3. Asymmetrical rolling of an AZ31 sheet

AZ31 samples, 2mm thick and 30mm wide, were rolled in symmetrical and asymmetrical conditions down to a final thickness of 1 mm. The as-received alloy exhibits a pronounced  $\{0002\}$  texture. The sheets were heated at 773K prior to reduction between cold rolls of identical size (180mm in diameter). The temperature was measured in situ with dedicated samples in which a thermocouple was introduced: it rapidly drops from 770K at the entry to 560K at the exit of the rolls. Three passes were imposed with roll speeds of 15 turns/min for the upper roll and 15 or 10 turns/min for the lower roll in case of symmetrical and asymmetrical rolling respectively. The cumulated shear strain promoted by the asymmetry of the roll speeds equals  $\gamma=0.8$ . Texture measurements performed in as-rolled conditions showed a departure from the basal texture after asymmetrical rolling similar to the one noticed previously [7]. This departure is a signature of the shear strain applied by the rolls due to their different rotation speeds.

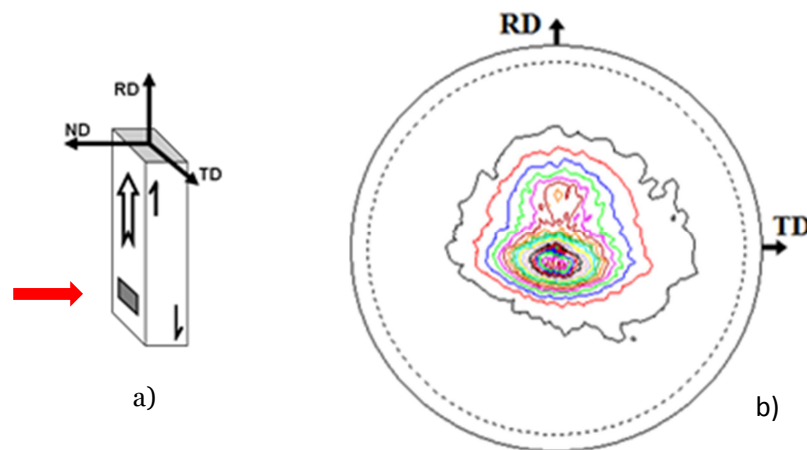


**Figure 2:**  $\{0002\}$  pole figure for the asymmetrically rolled AZ31 sheet. The main component is inclined 5 to 10° backward with respect to the rolling direction (RD). An additional component appears at ~30° in forward direction. The observation plane is perpendicular to the normal direction (ND) as shown in (a)

#### 4. Structural observations

The main observation mode in TEM is the bright field image: the structural features are highlighted by enhancing the contrast thanks to an aperture that rejects all diffracting beams except the transmitted ones. Such operating mode proves very useful for analyzing individual defects like stacking faults, dislocations or grain boundary. With plastic deformation, the density of defects increases tremendously. Consequently their contrasts combine, leading to hardly interpretable images. Figure 3 illustrate this difficulty by comparing a bright field image of a rolled sample and the corresponding orientation maps. Obviously, the multiple twins and grain boundaries appearing thanks to the color code are hidden in the bright field image. This limitation of conventional TEM observations prevents any proper characterization of severely deformed materials [8].

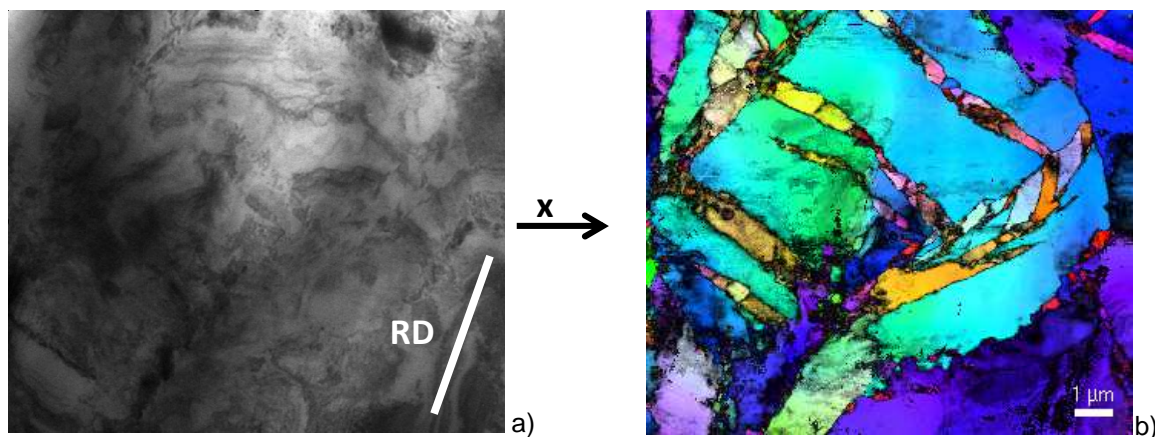


**Figure 3:** TD view of an AZ31 sheet highly deformed through asymmetrical rolling. Note the absence of details in the bright field image (a) while twins are easily detected on the orientation map (b). Most of them are double twins. The orientation map color code refers to x axis.

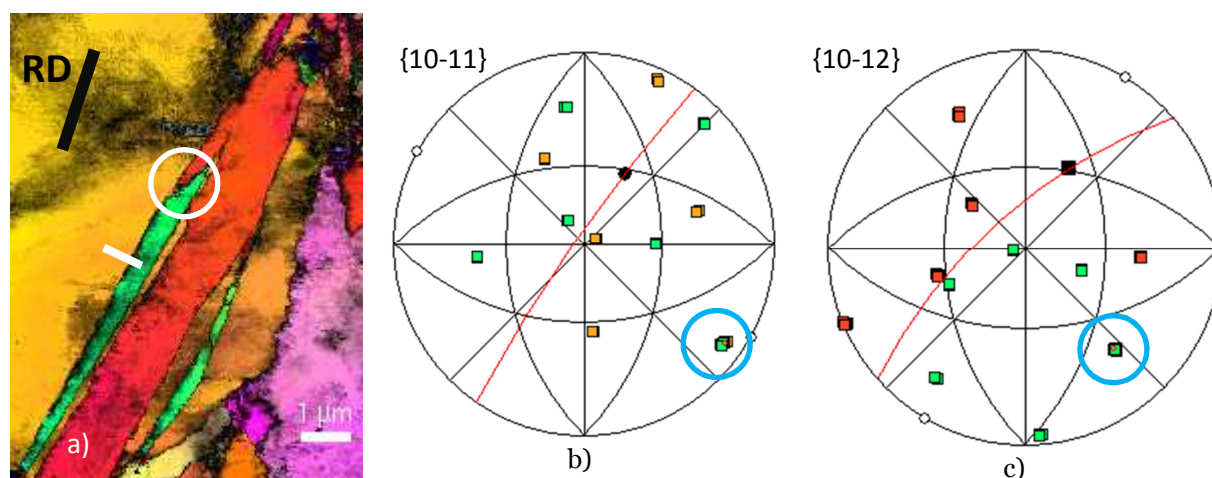
A spot diffraction pattern is less sensitive to strain than the bright field image. This is essentially related to the fact that all the beams are considered and not only the transmitted one. As for EBSD tools, the incident beam is focused and scanned over the area of interest in order to reconstruct step by step the orientation map.

Figure 3.b is a typical example of the inner structure of rolled AZ31. Numerous twins are observed. Several twin systems are expected (Table.1). Most of the twins are several microns long while the width is frequently less than one micron. Double twinning is frequent and requires a proper spatial resolution to be recognized unambiguously.

**Table I**: Primary and secondary twin commonly observed in magnesium and their frequency of appearance in conventional and asymmetrical rolling

Twin plane	Rotation axis	Twin direction	Disorientation	Frequency in conventional rolling	Frequency in asymmetrical rolling
{10-11}	<11-20>	<10-1-2>	56.2°	7%	34%
{10-12}	<11-20>	<10-1-1>	86.3°	67%	20%
{10-13}	<11-20>	<30-32>	64.0°	7%	6%
{10-11} - {10-12}	<11-20>		37.5°	11%	38%
{10-13} - {10-12}	<11-20>		29.7°	<2%	-

Twins were systematically indexed in order to analyze the relationship between the twin plane and shear orientation and the stress tensor associated to the rolling condition. Indexing a twin consists in (i) measuring the disorientation at the twin interface to select the possible twin system and (ii) plotting the adequate pole figure to confirm that the expected twin plane is a common plane. These two steps are illustrated in figure 4 in which a primary twin partially re-twinned is observed. The measured disorientation along the small white line crossing a primary twin boundary in Fig 4.a is  $\sim 55^\circ$  suggesting a {10-11} type twin. A common plane is recognized on the corresponding pole figure (circle in Fig 4.b). The trace of the common plane (red curve in Fig. 4.b) is reasonably aligned with the twin plane observed in Fig 4.a. Similarly, the disorientation between the primary twin and the secondary twin - surrounded by the circle in Fig.4.a - is  $\sim 86^\circ$ . A common plane appears on the {10-12} pole figure (Fig 4.c) whose trace is parallel to the twin plane observed on the orientation map.



**Figure 4:** {10-11} primary (white line) and {10-12} secondary twins (surrounded) in an asymmetrically rolled AZ31 sample. Twin systems are identified with the help of disorientation values (not shown) and pole figures that display the twin planes orientations (see text for details).

Over 20 scans have been performed – equally distributed on conventional and asymmetrically rolled thin foils - and more than 100 twins have been analyzed and practically all identified. Frequencies of appearance are given in Table I. There is a significant effect of the processing route on twinning in the magnesium alloy: the {10-12} twin system is dominant (2/3) for symmetrical rolling while the frequency is more distributed for asymmetrical rolling with frequent {10-11} - {10-12} double twins.

## 5. Twin activities

In the previous section, twinning has been reported to differ for conventional and asymmetrical rolling. This a priori suggests a direct impact of the shear component on the activity of the twin systems. The relationship between the stress tensors in rolling and twin system activities can be ascertained by considering the shear direction. Indeed, unlike slip systems, twins promote shear in a single and definite direction and consequently the sign of the applied stress may be inferred. A dedicated stereographic projection will be used to

examine this link (Fig. 5.c). In this plot the twin plane normal is marked at a location defined by the angle  $\alpha$  between the trace of the twin plane in the (ND, TD) plane and the rolling direction (Fig. 5.a) and the angle  $|\beta|$  that measures the deviation of the twin plane normal with respect to the (ND,RD) plane (Fig.5.b). As an example, the plan located at  $(\alpha,\beta)=(45^\circ;0^\circ)$  is marked by a triangle in Fig. 5.c. It corresponds to a highly stressed plane for conventional rolling. A deviation  $|\beta| > 0$  (note that the absolute value is used) will lower the applied stress in this plane.

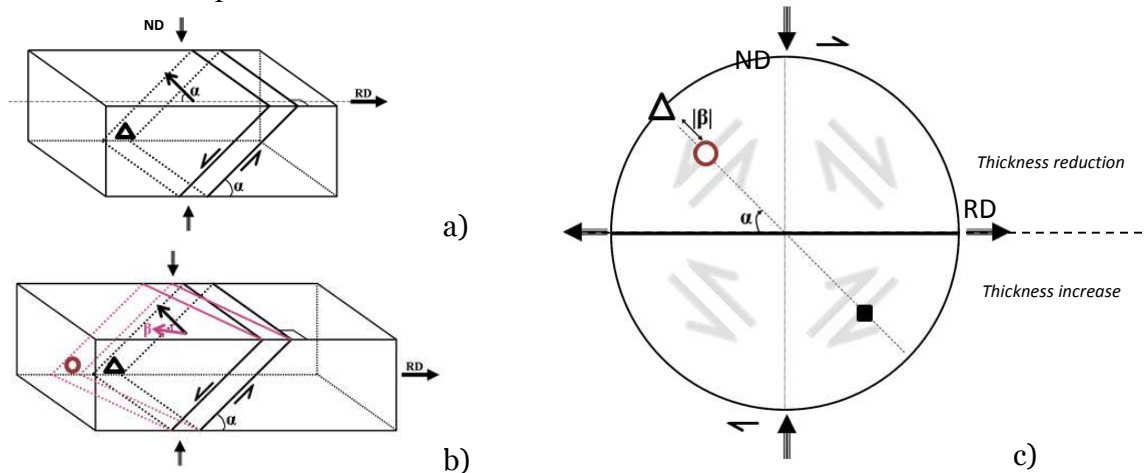


**Figure 5:** A stereographic representation of the twin plane in the rolling reference axes. The twin planes associated to coordinates  $(\alpha,0^\circ)$  and  $(\alpha,\beta)$  are drawn in (a) and (b) and the corresponding poles (triangle and circle) are plotted in (c). The upper and lower parts of the graph are used to distinguish twins which give rise either to a decrease or an increase (square) of the sheet thickness.

The objective of such construction will appear clearer with figures 6 et 7. In figure 6, the expected locations for twin planes are highlighted for conventional and asymmetrical rolling. In case of symmetrical rolling the maximum shear stress is applied on planes that are at  $\pm 45^\circ$  with respect to the rolling direction (i.e.:  $\alpha=45^\circ$  or  $135^\circ$ ). The additional shear promoted by the difference in roll speeds rotates these axes by a negative angle  $\theta$  whose amplitude depends on the ratio between the shear stress and normal stress. With the proposed projection, twins should appear only in the upper part of the stereographic projection, the lower part being associated to twins whose activity is in conflict with the thickness reduction expected from rolling.

The twin planes and shear direction measured on the orientation maps are computed in figure 7. The twin activity depends also on the shear direction. This direction is symbolized by the size of the marker that scale with the angle between the shear direction and the transverse direction: the largest symbol indicates that the shear direction is located in the (RD,ND) plane.

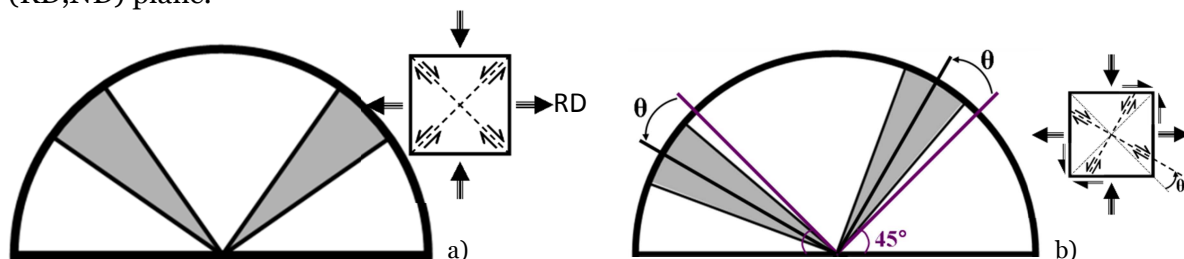


**Figure 6:** Upper hemisphere of the stereographic projection in which the expected location of twin planes is highlighted for a) conventional and b) asymmetrical rolling.

The results differ substantially with the rolling conditions. Some of the previously mentioned characteristics are easily noticed on the present projections: typically, it is evident that there is far more double twinning (open symbol) in asymmetrical rolling and that the main primary twins (solid symbol) appearing in conventional rolling is the  $\{10\text{-}12\}$  system (disks).

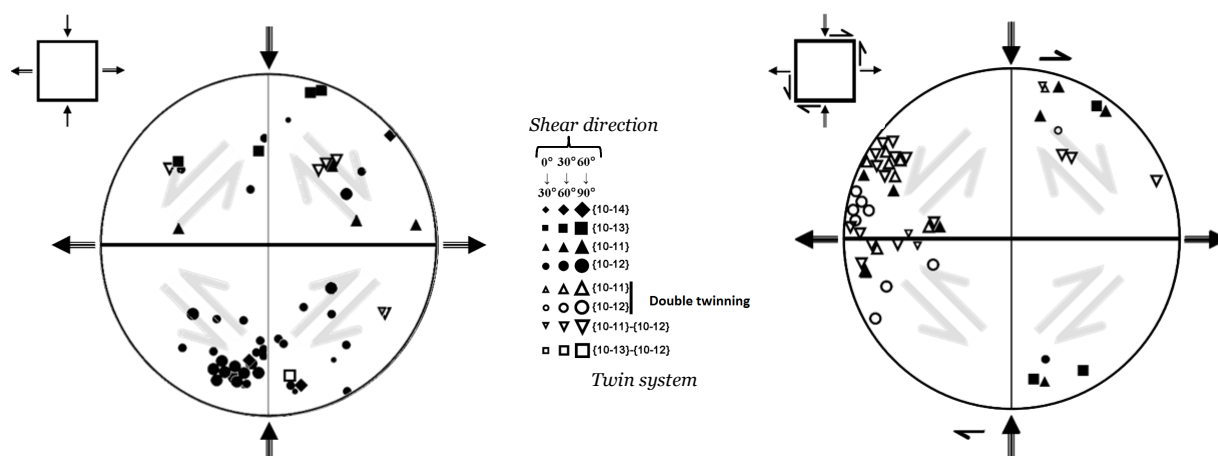


**Figure 7:** Stereographic projection of the location of twin planes a) conventional and b) asymmetrical rolling.

The most striking feature is the disagreement between the observed twin plane orientations (Fig. 7) and their expected locations (Fig. 6) for both symmetrical and asymmetrical rolling. In particular for conventional rolling, a large fraction of twins are placed in the lower hemisphere of the plot which means that their shear strain produces an increase of the thickness of the sample. It turns out that, owing to the main textural component of the sheet, most of these twins are ‘tensile’ twins while the stress tensor is of compressive type. A similar trend, although less pronounced, is observed for asymmetrical rolling. Such systematic observations may hardly be interpreted as some bias in, for example, thin-foil preparation. At the contrary, the definite signature of asymmetrical rolling (Fig. 7.b) with respect to symmetrical rolling (Fig. 7.a) denotes a strong effect of the deformation conditions on twin system activities. The existence of ‘tensile’ twins in rolling is surprising but not new. It was mentioned by Barnett et al [9] who concluded that their appearance is due to internal stresses that give rise to the activity of unexpected twin systems at unloading.

The additional input of the present work is related to the statistical view on twinning activities in asymmetrical conditions. As for conventional rolling, the activated planes are not oriented as derived from an ideal view of the stress tensor. By contrast, the distribution is not random. Most of the twins are located in well-defined sectors (Fig. 8.a). As for conventional rolling, a significant fraction of the twins are in the lower part of the graph that is associated to an increase of the sheet thickness. Of interest is the nearly symmetric distribution of these sectors that reminds the expected locations for simple shear (Fig. 8.b). Indeed, simple shear promotes activities in twin planes that are practically aligned with the horizontal or vertical axes in the figure, whatever the sign of the deviation from these ideal orientations. The direct comparison between shear type activities and observed activities suggests that the twins were more driven by the asymmetry of the rolling than by the thickness reduction. The possible reason for this similitude is that twinning occurs at the very end of the rolling process. At the exit of the rolls, the thickness reduction is practically achieved and shear resulting from the differential in tangential speeds at the roll surfaces become predominant. Moreover, the temperature of the sheet, which decreased dramatically due to the contact of the warm sample and the cold rolls, favor twinning activities at the end of process.

The main conclusion that is drawn from the previous facts is that twinning may appear as an important feature as far as structural observations are concerned but they play only a limited role in the forming process. Indeed, it was argued that they are activated mainly at unloading for conventional rolling [9] or at the exit of the rolls for asymmetrical rolling. Moreover, a crude estimate of the twin number and size gives a total volume of metal involved that is comprised between 5 and 25%. The twin strain is not more than 13%. Consequently, their contribution to strain is of the order of 0.05. This is to be compared to the 0.8 equivalent

strain promoted by a 50% reduction in conventional rolling (0.9 for asymmetrical rolling). Besides, it has been ascertain that the texture component specific of asymmetrical rolling (Fig. 2) is not due to the change in orientation of the twinned volume.

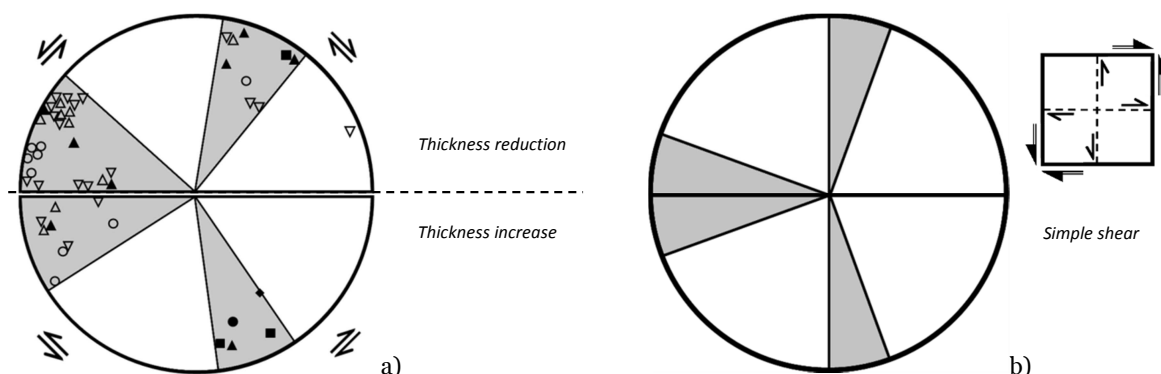


**Figure 8:** Stereographic projection of the location of twin planes a) asymmetrical rolling and b) as expected in simple shear.

## 6. Conclusions

An Automated Crystal Orientation Mapping (ACOM) facility is used to analyze TEM thin foils of AZ31 sheets deformed in conventional and asymmetrical rolling. Numerous primary and secondary twins are easily noticed and characterized with the help of the orientation maps. Their frequency and type depend on the processing route. Numerous twins have an orientation that is not compatible with the stress tensor pertaining to rolling. It is claimed that they mainly appear at the exit of the rolls. Consequently, the formability during rolling is not related to the twin systems activity and distribution.

## References

- [1] Huang X Suzuki K Watazu A Shigematsu I Saito N. Improvement of formability of Mg–Al–Zn alloy sheet at low temperatures using differential speed rolling. *J Alloy Compd* 2009;470:263-268
- [2] Rauch E F Portillo J Nicolopoulos S Bultreys D Rouvimov S and Moeck P 2010 *Zeitschrift für Kristallographie* **225** issue 2-3 103
- [3] Schwarzer R A and Sukkau J 1998 *Materials Science Forum* **273-275** 215
- [4] Fundenberger J J Morawiec A Bouzy E Lecomte J S 2003 *Ultramicroscopy* **96** 127
- [5] Rauch E F and Dupuy L 2005 *Arch. Metall. Mater* **50** 87
- [6] Rauch E F and Véron M 2005 *J. Mater. Sci. Eng. Tech.* **36** 552
- [7] Huang X Suzuki K Watazu A Shigematsu I Saito N 2008 *Mater. Sci. and Eng.* **A488** 214
- [8] Rauch E F and Véron M 2012 *Proc Int. Symp. on Plastic Deformation and Texture Analysis* Ed. Amigo Borrás V Alcoy (Spain) pp 119-209
- [9] Barnett M R Nave M D Bettles C J 2004 *Mater. Sci. and Eng.* **A386** 205